NATIONAL ADVISORY COMMITTEE FOR AERONAUTICS

TECHNICAL NOTE 2492

A METHOD OF SOLVING THE DIRECT AND INVERSE PROBLEM OF SUPERSONIC FLOW ALONG ARBITRARY STREAM FILAMENTS OF REVOLUTION IN TURBOMACHINES

By Chung-Hua Wu and Eleanor L. Costilow

Lewis Flight Propulsion Laboratory
Cleveland, Ohio

Washington
September 1951

NATIONAL ADVISORY COMMITTEE FOR AERONAUTICS

TECHNICAL NOTE 2492

A METHOD OF SOLVING THE DIRECT AND INVERSE PROBLEM OF SUPERSONIC FLOW ALONG ARBITRARY STREAM FILAMENTS OF REVOLUTION IN TURBOMACHINES

By Chung-Hua Wu and Eleanor L. Costilow

SUMMARY

Analysis of the supersonic flow in two two-dimensional high-solidity cascades and in a partly supersonic symmetrical nozzle shows that there is, in general, significant deviation of the mean streamline shape from that of the mean blade line and that the effect of blade thickness and blade curvature on the specific mass flow along the mean streamline is to increase the specific mass flow along the mean streamline about 9 percent above that given by a one-dimensional estimate. In order to determine these effects more accurately for turbomachines of arbitrary hub and casing shapes to be used for the three-dimensional through-flow calculation, a method is developed for the determination of the supersonic flow along stream surfaces of revolution in turbomachines. In this method, the shapes of the stream surfaces are arbitrary, and the method also takes into account the distance between adjacent stream surfaces, which varies along the flow path. Thus, the method can be applied to turbomachines with arbitrary hub and casing shapes.

In addition to their use for direct problems, these equations can be used to design blade elements in supersonic flow along an arbitrary stream filament of revolution in turbomachines.

INTRODUCTION

Recent investigations of the applicability of supersonic flow in compressors have shown the desirability of using such flow to increase the pressure ratio per stage (references 1 and 2). For axial-flow compressors having blades with short radial length, the over-all performance analysis is often based on a one-dimensional approximation, in which only average values in the channel are considered (for example, references 3 and 4). For radially long blades and variable root or tip radii, methods are proposed for analyzing the flow by a three-dimensional "through-flow" calculation, which considers the axial and

radial variations of the flow but only a mean value in the circumferential direction (references 5 and 6). The flow on the relative mean stream surface, which divides circumferentially the mass flow passing through the channel between two blades into two equal parts, is taken to represent the mean flow through the blading. It is suggested in reference 5 that the shape of this mean stream surface and the correction factor b for a finite number of thick blades be obtained from the analysis of a number of two-dimensional flows along general surfaces of revolution starting at different inlet radii. A method was therefore developed at the NACA Lewis laboratory to determine the flow variation on these flow surfaces in a supersonic turbomachine. When the flow surfaces may be approximated by cylindrical surfaces, the flow equations reduce to the usual plane flow where the hodograph characteristics are applicable for the flow analysis if the entrance shock is weak.

In order to illustrate the effects of blade thickness and blade curvature and to determine, in general, the correlation between the shapes of the mean streamline and the mean blade line, flow on the mean streamlines was determined for two supersonic cascades and a partly supersonic hyperbolic nozzle.

This method, in addition to its use for flow analysis of a given blading, can be used to design blade elements along stream filaments of revolution having arbitrary thickness variation along the flow path.

SYMBOLS

The following symbols were used in this report:

A	area normal to velocity
a	local speed of sound
b	correction factor for finite number of thick blades
c	line tangent to characteristic curve
c_p	specific heat at constant pressure
h	static enthalpy
I	$h + \frac{1}{2}w^2 - \frac{1}{2}\omega^2 r^2$
J,K,L M,N	coefficients of partial derivatives of ψ

l,φ	orthogonal coordinates on mean surface of revolution
M	local Mach number
m	mass flow between suction surface of blade and streamline, $\int_0^{\xi} \rho W \, d\xi$
P	blade pitch or spacing
R	gas constant
r	radial distance from axis of machine (fig. 1)
s	entropy
T	static temperature
t	blade thickness in the y-direction
W	resultant relative velocity
x,y	rectangular coordinates for cylindrical flow with y-axis chosen along line joining leading edges of blade
β	relative flow angle, $\tan^{-1} \frac{W_\varphi}{W_l}$
γ	ratio of specific heats
λ	slope of characteristics on mean surface of revolution
μ	Mach angle, $\sin^{-1} \frac{1}{M}$
ξ	distance measured from suction to pressure surface normal to resultant velocity
ρ	mass density
σ	slope of mean surface of revolution in meridional plane, $\tan^{-1} \frac{W_r}{W_z}$
τ	normal thickness of stream filament of revolution
ψ	stream function

ω angular velocity of blade

Subscripts:

i inlet condition

l,φ meridional and circumferential components

m on mean streamline

r,z components in r- and z-directions, respectively

s initial supersonic state

t at throat of nozzle

x,y components along x- and y-directions, respectively

1,2 first and second family of characteristics, respectively

METHOD

On a general surface of revolution defined by the orthogonal coordinates l and φ (figs. 1(a) to 1(c)), the supersonic flow of a fluid along a stream filament of revolution of varying normal thickness $\tau = \tau(l)$ is described by the following forms of the flow equations. By analyzing the flow going in and out of the element shown in figure 1(d), the continuity equation for steady flow may be expressed by

$$\frac{\partial(\tau\rho W_l r)}{\partial l} + \frac{\partial(\tau\rho W_\varphi)}{\partial \varphi} = 0 \tag{1}$$

When equation (1) is expanded and the relation

$$d \ln \rho = \frac{dh}{a^2} - d\left(\frac{s}{R}\right)$$

is used, equation (1) becomes

$$\frac{\partial}{\partial l}(W_l \tau r) + \frac{\partial}{\partial \varphi}(\tau W_\varphi) + \frac{\tau}{a^2}\left(W_l r \frac{\partial h}{\partial l} + W_\varphi \frac{\partial h}{\partial \varphi}\right) - \frac{\tau}{R}\left(W_l r \frac{\partial s}{\partial l} + W_\varphi \frac{\partial s}{\partial \varphi}\right) = 0 \tag{2}$$

For adiabatic flow, the entropy along a streamline remains constant for a nonviscous fluid; that is

$$\frac{Ds}{Dt} = W_l \frac{\partial s}{\partial l} + \frac{W_\varphi}{r} \frac{\partial s}{\partial \varphi} = 0$$

which allows the last term to be dropped from equation (2). For a perfect gas,

$$h = c_p T$$

and

$$a^2 = (\gamma - 1)\, h$$

When this substitution is made for a^2 and the expression is multiplied by $h^{\frac{1}{\gamma-1}}$, the equation of continuity (2) becomes:

$$\frac{\partial}{\partial l}\left(\tau W_l r h^{\frac{1}{\gamma-1}}\right) + \frac{\partial}{\partial \varphi}\left(\tau W_\varphi h^{\frac{1}{\gamma-1}}\right) = 0 \qquad (3)$$

Expressed in the coordinates l and φ, the equation of steady motion of a nonviscous fluid as given by equation (14a) in reference 5 in the circumferential direction, is

$$\frac{1}{r}\frac{\partial W_l}{\partial \varphi} - \frac{\partial W_\varphi}{\partial l} - \left(\frac{W_\varphi}{r} + 2\omega\right)\sin\sigma - \frac{1}{W_l}\left(\frac{I}{r}\frac{\partial I}{\partial \varphi} - \frac{T}{r}\frac{\partial s}{\partial \varphi}\right) = 0 \qquad (4)$$

From equation (3), a stream function ψ is defined by:

$$\frac{\partial \psi}{\partial \varphi} = r\tau W_l h^{\frac{1}{\gamma-1}} \qquad (5a)$$

$$\frac{\partial \psi}{\partial l} = -\tau W_\varphi h^{\frac{1}{\gamma-1}} \qquad (5b)$$

Substituting equations (5) into equation (4) results in the following relation:

$$\left(1 - \frac{W_l^2}{a^2}\right)\frac{\partial^2\psi}{\partial l^2} - 2\frac{W_l W_\varphi}{a^2}\frac{1}{r}\frac{\partial^2\psi}{\partial\varphi\,\partial l} + \left(1 - \frac{W_\varphi^2}{a^2}\right)\frac{1}{r^2}\frac{\partial^2\psi}{\partial\varphi^2} -$$

$$\frac{1}{a^2}\left[\left(\omega^2 r + \frac{W_l^2}{r}\right)\sin\sigma + \frac{a^2}{\tau}\frac{\partial\tau}{\partial l} + \frac{\partial I}{\partial l}\right]\frac{\partial\psi}{\partial l} -$$

$$\left\{\left(1 - \frac{W^2}{a^2}\right)\left[\left(\frac{W_\varphi}{r} + 2\omega\right)\frac{\sin\sigma}{W_l} + \frac{1}{W_l^2}\left(\frac{1}{r}\frac{\partial I}{\partial\varphi} - \frac{T}{r}\frac{\partial s}{\partial\varphi}\right)\right] + \frac{1}{a^2 r}\frac{\partial I}{\partial\varphi}\right\}\frac{1}{r}\frac{\partial\psi}{\partial\varphi} = 0 \tag{6}$$

If the symbols J, K, L, M, and N are used to represent the coefficients of the partial derivatives in equation (6), it may be rewritten as

$$J\frac{\partial^2\psi}{\partial l^2} + \frac{2K}{r}\frac{\partial^2\psi}{\partial\varphi\,\partial l} + \frac{L}{r^2}\frac{\partial^2\psi}{\partial\varphi^2} + M\frac{\partial\psi}{\partial l} + \frac{N}{r}\frac{\partial\psi}{\partial\varphi} = 0 \tag{7}$$

The characteristics of equation (7) are then

$$J\left(r\frac{d\varphi}{dl}\right)^2 - 2K\left(r\frac{d\varphi}{dl}\right) + L = 0 \tag{8}$$

For equation (8), two real characteristics exist for supersonic flow, the slopes along which are

$$\lambda_1 = \left(r\frac{d\varphi}{dl}\right)_1 = \frac{K}{J} - \frac{\sqrt{K^2 - JL}}{J} \tag{9a}$$

$$\lambda_2 = \left(r\frac{d\varphi}{dl}\right)_2 = \frac{K}{J} + \frac{\sqrt{K^2 - JL}}{J} \tag{9b}$$

When the polar coordinates transformation that $\beta = \tan^{-1}\frac{W_\varphi}{W_l}$ and $\mu = \sin^{-1}\left(\frac{1}{M}\right) = \sin^{-1}\left(\frac{a}{W}\right) = \sin^{-1}\frac{a}{\sqrt{W_l^2 + W_\varphi^2}}$ is used, the relation of λ to the flow angle and the Mach angle is

$$\lambda_1 = \tan (\beta + \mu) \tag{10a}$$

$$\lambda_2 = \tan (\beta - \mu) \tag{10b}$$

By the use of equations (7) and (9), the rate of change of ψ-derivatives along the characteristics with respect to l is obtained (see reference 5 for procedure): Along c_1,

$$\frac{d}{dl}\left(\frac{\partial\psi}{\partial l}\right) + \frac{\lambda_2}{r}\frac{d}{dl}\left(\frac{\partial\psi}{\partial\varphi}\right) + \frac{M}{J}\frac{\partial\psi}{\partial l} + \frac{N}{Jr}\frac{\partial\psi}{\partial\varphi} = 0 \tag{11a}$$

and along c_2

$$\frac{d}{dl}\left(\frac{\partial\psi}{\partial l}\right) + \frac{\lambda_1}{r}\frac{d}{dl}\left(\frac{\partial\psi}{\partial\varphi}\right) + \frac{M}{J}\frac{\partial\psi}{\partial l} + \frac{N}{Jr}\frac{\partial\psi}{\partial\varphi} = 0 \tag{11b}$$

For ease in computation, it is more convenient to express equations (11) in terms of the magnitude of the resultant velocity W and the flow angle β as follows: Substituting equations (5) in equations (11) and differentiating yields the following expression along c_1:

$$(\lambda_2 W_l - W_\varphi)\frac{\tau}{a^2}\frac{dh}{dl} + \tau\left(\lambda_2\frac{dW_l}{dl} - \frac{dW_\varphi}{dl}\right) + (\lambda_2 W_l - W_\varphi)\frac{d\tau}{dl} +$$

$$\frac{\tau}{J}(NW_l - MW_\varphi) + \frac{\lambda_2}{r}\tau W_l \sin\sigma = 0$$

Similarly, along c_2,

$$(\lambda_1 W_l - W_\varphi)\frac{\tau}{a^2}\frac{dh}{dl} + \tau\left(\lambda_1\frac{dW_l}{dl} - \frac{dW_\varphi}{dl}\right) + (\lambda_1 W_l - W_\varphi)\frac{d\tau}{dl} +$$

$$\frac{\tau}{J}(NW_l - MW_\varphi) + \frac{\lambda_1}{r}\tau W_l \sin\sigma = 0$$

With

$$W_l = W \cos \beta$$

$$W_\varphi = W \sin \beta$$

and

$$\frac{dh}{dl} = \frac{d}{dl}\left(I - \frac{W^2}{2} + \frac{\omega^2 r^2}{2}\right) = \frac{dI}{dl} - W\frac{dW}{dl} + \omega^2 r \sin \sigma$$

and with the use of equations (10), equations (11) become

$$\frac{1}{W}\frac{dW}{dl} - \tan \mu \frac{d\beta}{dl} - \tan^2 \mu \left[\frac{\omega^2 r \sin \sigma}{a^2} + \frac{1}{a^2}\frac{dI}{dl} + \frac{1}{\tau}\frac{d\tau}{dl} + \frac{\lambda_2 \sin \sigma \cos \beta}{r(\lambda_2 \cos \beta - \sin \beta)} + \frac{1}{J}\frac{N \cos \beta - M \sin \beta}{(\lambda_2 \cos \beta - \sin \beta)}\right] = 0 \tag{12a}$$

$$\frac{1}{W}\frac{dW}{dl} + \tan \mu \frac{d\beta}{dl} - \tan^2 \mu \left[\frac{\omega^2 r \sin \sigma}{a^2} + \frac{1}{a^2}\frac{dI}{dl} + \frac{1}{\tau}\frac{d\tau}{dl} + \frac{\lambda_1 \sin \sigma \cos \beta}{r(\lambda_1 \cos \beta - \sin \beta)} + \frac{1}{J}\frac{N \cos \beta - M \sin \beta}{(\lambda_1 \cos \beta - \sin \beta)}\right] = 0 \tag{12b}$$

along c_1 and c_2, respectively.

From two points a and b (fig. 2) where the flow is known, the tangents to the characteristics curves at these points are determined from equations (9a) and (9b), respectively, and intersect at a point c. By writing equation (12a) (equation along c_1) at a and equation (12b) (equation along c_2) at b in finite difference form and solving simultaneously, the new flow values at c are determined; thus, along c_1 at a,

$$\frac{1}{W_a}\frac{W_c - W_a}{l_c - l_a} - \tan \mu_a \frac{\beta_c - \beta_a}{l_c - l_a} - \tan^2 \mu_a \frac{\omega^2 r \sin \sigma_a}{a^2} + \ldots \tag{13}$$

and along c_2 at b,

$$\frac{1}{W_b}\frac{W_c - W_b}{l_c - l_b} + \tan \mu_b \frac{\beta_c - \beta_b}{l_c - l_b} - \tan^2 \mu_b \frac{\omega^2 r \sin \sigma_b}{a^2} + \ldots \tag{14}$$

The unknowns in both equations (13) and (14) are W_c and β_c; Δl is determined by the intersection of the tangents to the characteristics from points a and b so that $l_c - l_a$ and $l_c - l_b$ are known in the equation.

For a characteristic curve that intersects the passage boundary, such as is shown at d or e in figure 2, the situation is a little different. In a direct problem with a given blade configuration, the angle β at the intersecting boundary point is known. In the inverse or blade-design problem, either β at the intersecting boundary point is known from a desirable turning specified at that point or the magnitude of the resultant velocity W at the intersecting boundary point is known from a specified velocity distribution on the blade. In all cases, either equation (13) or (14) written for the characteristic from d or e determines the unknown W or β at the intersecting boundary point, whereas, as shown previously, two simultaneous equations along intersecting characteristics are required inside the passage. In general, after W and β are determined at a new point, other fluid properties at that point are calculated and the characteristic directions constructed to repeat the process progressively downstream. (For irrotational inlet flow with uniform I and s and when the rotationality introduced by the entrance shocks is neglected, I and s are uniform throughout for adiabatic flow, and the derivatives involved in equations (12) become zero. Otherwise, the derivatives are to be evaluated by using the values at the inlet on different streamlines, the constancy along the streamline before and after shock, and the changes across the shock.)

Thus a method is available either to analyze the blade-to-blade flow variation along a given arbitrary stream filament of revolution in a supersonic turbomachine, or to design the blade element on a given arbitrary stream filament of revolution for a specified turning distribution or a specified velocity distribution around the blade. The configuration of the stream filaments (fig. 1(a)) is taken from a through-flow calculation (references 5 and 6). For a direct problem, successive calculations between the through-flow calculation and the present calculation are necessary until the solution converges. The through-flow calculation gives the configuration of stream filaments of revolution, and the calculation on these stream filaments of revolution gives the shape of the mean stream surface and the factor b used in reference 5, which accounts for the effect of blade thickness and curvature. In an inverse problem, the calculation is shortened if the estimated values of the factor b used in the through-flow calculation for a desirable blade-thickness distribution results in a blade dimension which has a thickness distribution close enough to the desirable one.

In order to give a general idea of the order of magnitude of this factor b for the effect of the blade thickness and curvature on the mean flow and the closeness of the shape of the mean stream surface to the blade mean surface, an analysis is made for the simpler case of cylindrical flow utilizing available data for two two-dimensional high-solidity cascade recently investigated by Liccini at the NACA Langley laboratory (unpublished data) and for a partly supersonic nozzle investigated by Emmons (reference 7).

ANALYSIS OF FLOW IN TWO SUPERSONIC CASCADES AND ONE PARTLY SUPERSONIC NOZZLE

The shapes of the two high-solidity 90° turning-angle cascades are shown in figure 3. Each cascade has an inlet Mach number of 1.78 and a 10° wedge angle at the leading edge. (The blade is so designed that the leading-edge shock is cancelled after the first reflection.) The shape of the partly supersonic nozzle is shown in figure 4. (Because the nozzle is symmetrical, only half of it is shown.)

In the case of the symmetrical nozzle, the center line is the mean streamline. For the two 90° cascades, the mean streamline (the one which divides the mass flow in the channel into two equal parts) has to be established from the data given on the characteristic net of the blade design. The mass flow m at any point in the channel is determined by integrating across the channel the local specific mass flow given by the characteristic net; thus, $m = \int_0^{\xi} \rho W \, d\xi$. The values of the local specific mass flow can be obtained by using the table given in reference 8 or similar tables. The shape of the mean streamline is to be compared with that of the mean blade line, which is obtained by taking the mean of the blade coordinates in the pitch direction.

The value of the specific mass flow W or W_x is then obtained along the mean streamline downstream of its intersection with the leading-edge shock. The discontinuity in the flow curves at the point where the mean streamline intersects the "reflection" is smoothed out in order to emphasize the general trend. These values are to be compared with the corresponding variation in the channel width (or area) perpendicular to W or W_x in order to determine if there is any correlation between the variations in specific mass flow on the mean streamline and the corresponding area.

In the case of the nozzle, the flow variation on the mean streamline is obtained from the Mach number given in reference 7. The variation in specific mass flow is compared with the channel-area ratio.

The results obtained in the two 90° turning passages are given in figures 3 and 5 to 9. The results obtained with the symmetrical nozzle are shown in figures 4, 10, and 11.

In figures 3(a) and 3(b), the mean streamline is compared with the mean channel line. In figure 3(a), where the cascade is of the higher solidity and has thinner blades, the shape of the mean streamline closely approximated that of the mean camber line; however, in the second cascade (fig. 3(b)), which has a lower solidity and thicker blades, the mean streamline deviates more from the mean blade line.

The specific mass flow on the mean streamline based on the resultant velocity as shown in figure 5 indicates clearly that the effect of blade thickness and curvature on the through flow is to increase, in both cases investigated, the specific mass flow along the mean streamline a chordwise average of 9 percent over that given by the area reduction (due to blade thickness) based on a one-dimensional calculation. If a comparison of specific mass flow in the axial direction with variation of channel width in the y-direction is made (fig. 6), as is done in reference 9 for subsonic flow, corresponding trends are obtained, and the increase in specific mass flow again averages about 9 percent chordwise over the area ratio. This increase is more than two times the increase obtained in reference 9.

The variations of axial and tangential velocity components on the mean streamline are shown in figures 7 and 8, respectively. The variations of the velocity across the channel in the two cascades at the stations indicated on figure 3 are shown in figure 9.

The result obtained in the nozzle problem is shown in figures 10 and 11. The results shown in figure 10 correspond to the nozzle shown in figure 15 of reference 7, which includes a small portion of supersonic flow in the divergent portion of the nozzle; whereas figure 11 corresponds to figure 16 of reference 7, with supersonic flow extending throughout the divergent portion and the Mach number increasing beyond 2. For the subsonic flow in the convergent portion, the local specific mass flow and area are normalized by the values at the throat; for the flow in the divergent portion (partly supersonic, fig. 8, and purely supersonic, fig. 9), the local specific mass flow and area are normalized with respect to the conditions where the flow is initially supersonic. The comparison between the specific mass flow and area ratio is similar to the previous result. The increase in the specific mass flow on the mean streamline is entirely due to the area reduction (no turning) and is about 8 percent higher than a one-dimensional correction.

The results obtained in these analyses give some idea regarding the closeness between the shape of the blade mean line and mean streamline and of the order of magnitude of the blade thickness and curvature effect for through-flow calculations. For an approximate through-flow solution of a similar blading, these results may be directly applied. For different types of blading, similar analyses can be made for the two-dimensional flow on cylindrical surfaces or surfaces of revolution, which are formed by fluid particles initially lying on circular arcs at a number of radii upstream of the machine by using the general relations derived herein. The mean streamline obtained at the different radii can be joined together to form the mean stream surface. The ratio of $(\rho W_x)_m$ to $(\rho W_x)_i$ obtained in these calculations can be taken as the thickness correction factor b in the relations between stream function and velocities (equation (111) of reference 5).

More knowledge of this kind for a number of typical bladings will be very useful in the design of these bladings. From this knowledge and a certain blade-thickness distribution, which is desired from the blade strength and other considerations, a good estimate of the factor b can be made and used in the through-flow calculation. From this solution, the blade section on a number of surfaces of revolution can be designed by the method given in the report.

SUMMARY OF RESULTS

Analysis of the supersonic flow in two two-dimensional 90° turning passages of high solidity and in a partly supersonic symmetrical nozzle shows that there is, in general, significant deviation of the mean streamline shape from that of the mean blade line and that the effect of blade thickness and blade curvature on the specific mass flow along the mean streamline is to increase the specific mass flow along the mean streamline about 9 percent above that given by a one-dimensional estimate. In order to determine these effects more accurately for turbomachines of arbitrary hub and casing shapes to be used for the three-dimensional through-flow calculations, a method is developed for the determination of the supersonic flow along stream surfaces of revolution in turbomachines. In this method the shapes of the stream surfaces are arbitrary, and the method also takes into account the distance between adjacent stream surfaces, which distance varies along the flow path. Thus, the method can be applied to turbomachines with arbitrary hub and casing shapes.

In addition to their use for direct problems, these equations can be used to design blade elements in supersonic flow along an arbitrary stream filament of revolution in turbomachines.

Lewis Flight Propulsion Laboratory
National Advisory Committee for Aeronautics
Cleveland, Ohio, July 13, 1951

REFERENCES

1. Weise, A.: A Supersonic Axial Compressor. TPA3/TIB Trans. No. GDC 10/6116T, British M.O.S., Oct. 1943.

2. Kantrowitz, Arthur: The Supersonic Axial-Flow Compressor. NACA Rep. 974, 1950. (Formerly ACR L6D02.)

3. Wattendorf, Frank L.: High-Speed Flow Through Cambered Rotating Grids. Jour. Aero. Sci., vol. 15, no. 4, April 1948, pp. 243-247.

4. Loeb, W. A.: A Study of the Supersonic Axial-Flow Compressor. Jour. Appl. Mech., vol. 16, no. 1, March 1949, pp. 19-26.

5. Wu, Chung-Hua: General Through-Flow Theory of Fluid Flow with Subsonic or Supersonic Velocity in Turbomachines of Arbitrary Hub and Casing Shapes. NACA TN 2302, 1951.

6. Goldstein, Arthur W.: Axisymmetric Supersonic Flow in Rotating Impellers. NACA TN 2388, 1951.

7. Emmons, Howard W.: The Theoretical Flow of a Frictionless, Adiabatic, Perfect Gas Inside of a Two-Dimensional Hyperbolic Nozzle. NACA TN 1003, 1946.

8. Burcher, Marie A.: Compressible Flow Tables for Air. NACA TN 1592, 1948.

9. Wu, Chung-Hua, and Brown, Curtis A.: Method of Analysis for Compressible Flow Past Arbitrary Turbomachine Blades on General Surface of Revolution. NACA TN 2407, 1951.

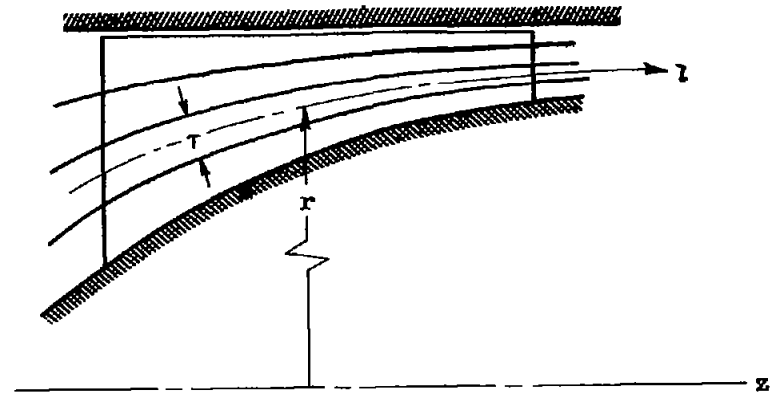

(a) Streamline in meridional plane.

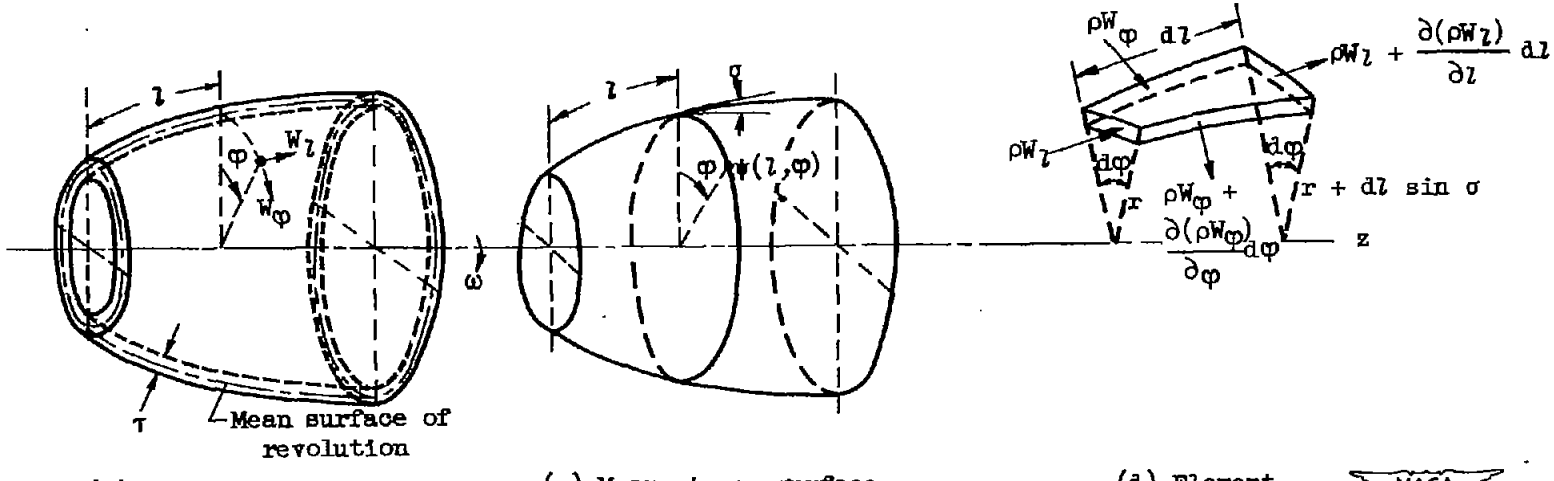

(b) Stream filament of revolution.

(c) Mean stream surface of revolution.

(d) Element.

Figure 1. - Flow on stream filament of revolution and surface of revolution.

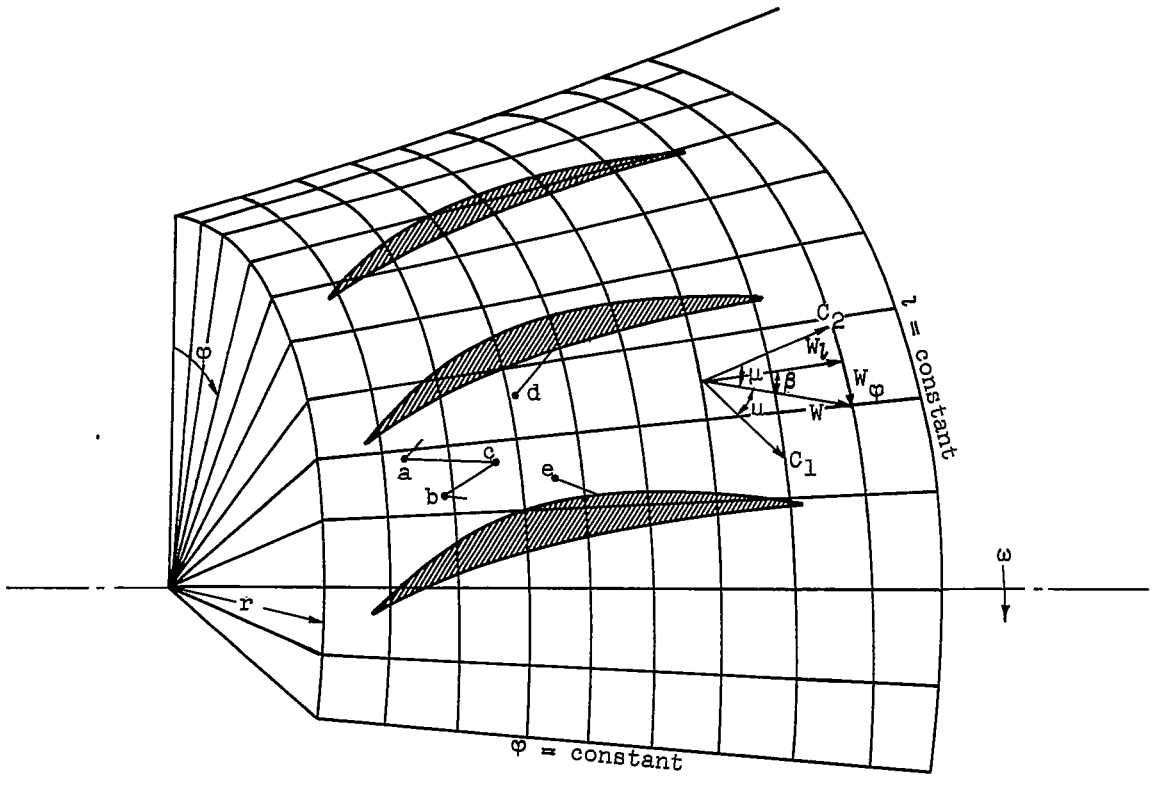

(a) On mean surface of revolution.

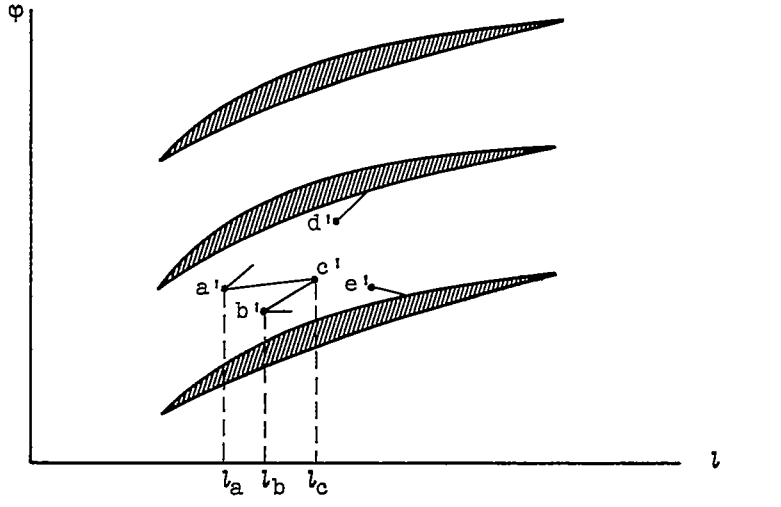

(b) Image in l,φ plane.

Figure 2. - Blade section and calculating points.

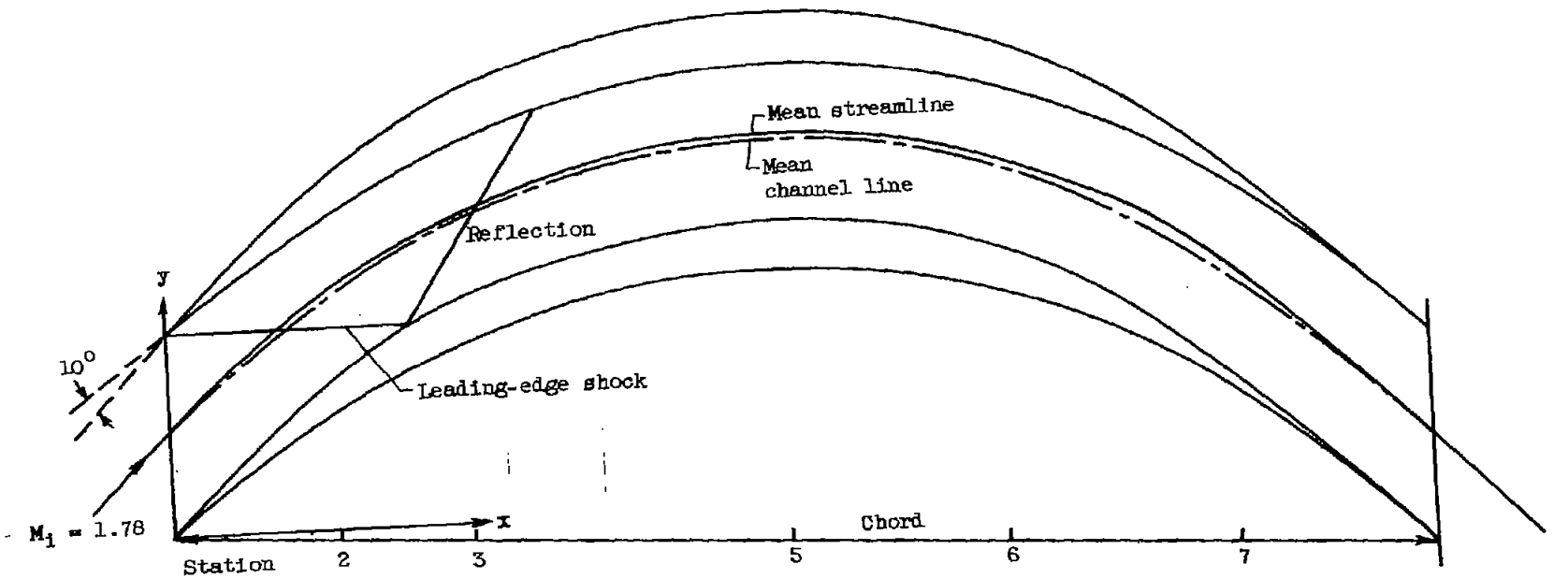

(a) Case a.

Figure 3. - Comparison of mean streamline and mean channel line in supersonic cascades.

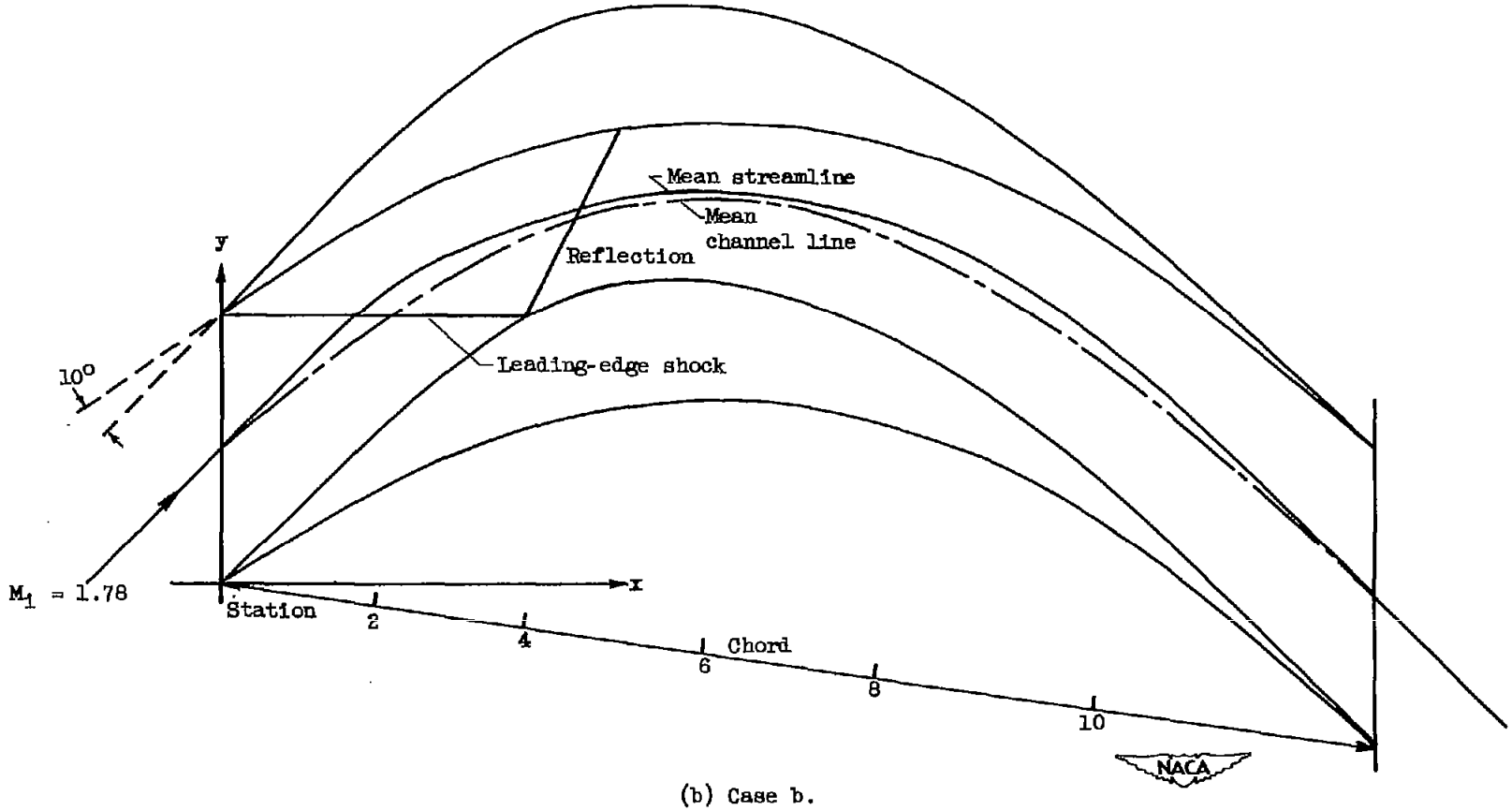

(b) Case b.

Figure 3. - Concluded. Comparison of mean streamline and mean channel line in supersonic cascades.

Figure 4. - Hyperbolic nozzle.

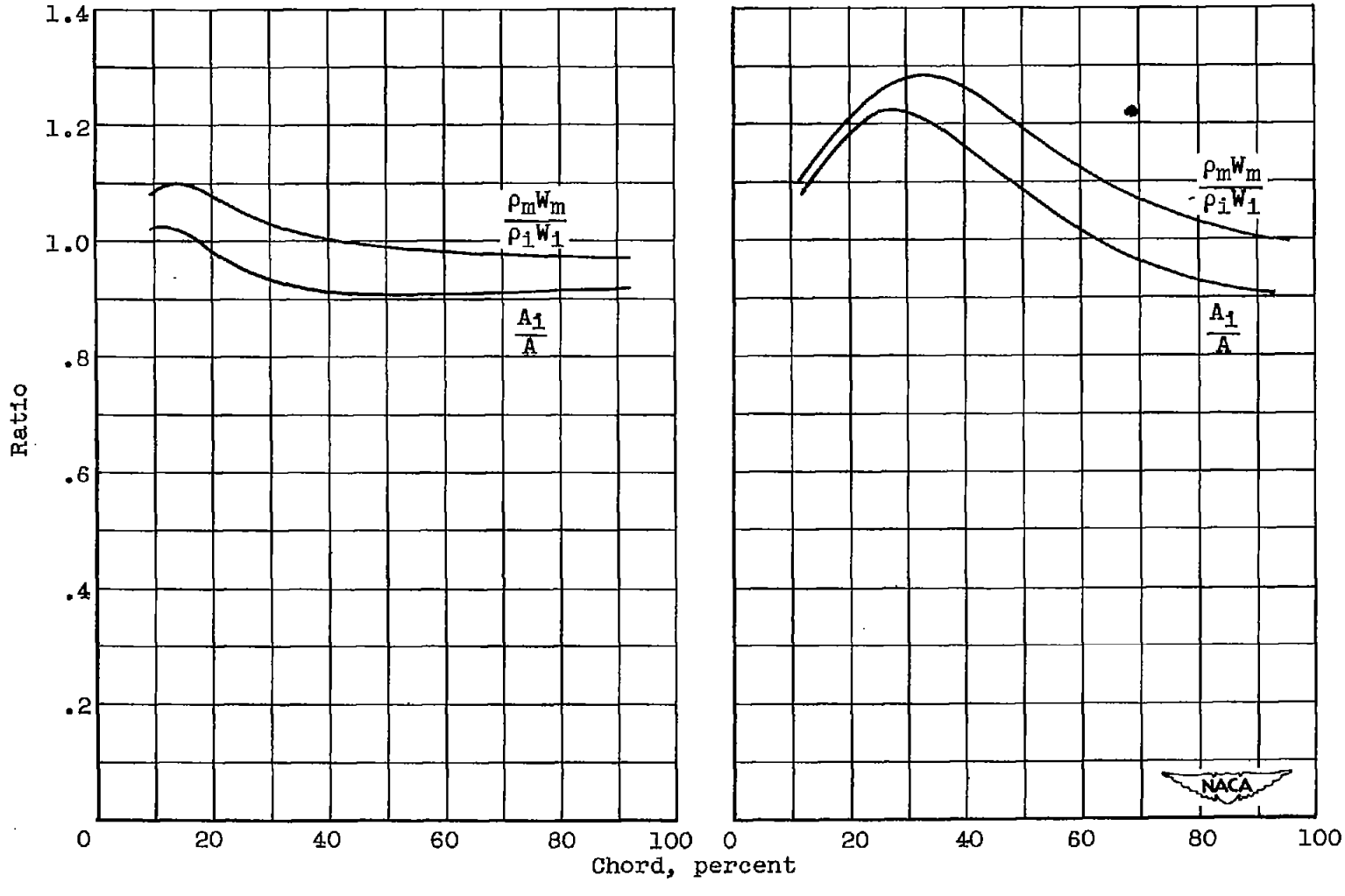

(a) Case a.

(b) Case b.

Figure 5. - Comparison between variations of specific mass flow on mean streamline and normal channel area ratio.

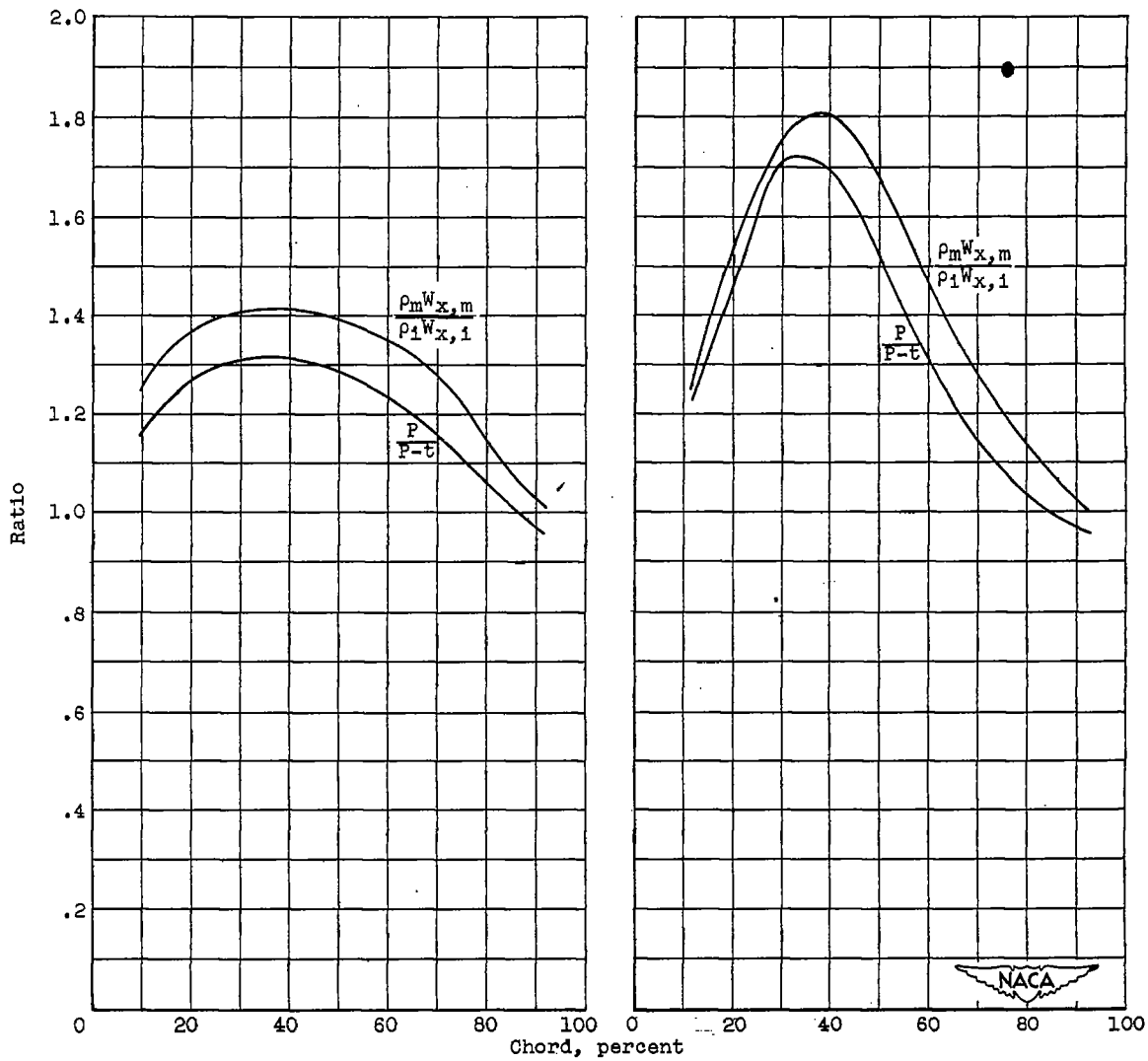

(a) Case a. (b) Case b.

Figure 6. - Comparison of specific mass flow in x-direction with channel area ratio in y-direction.

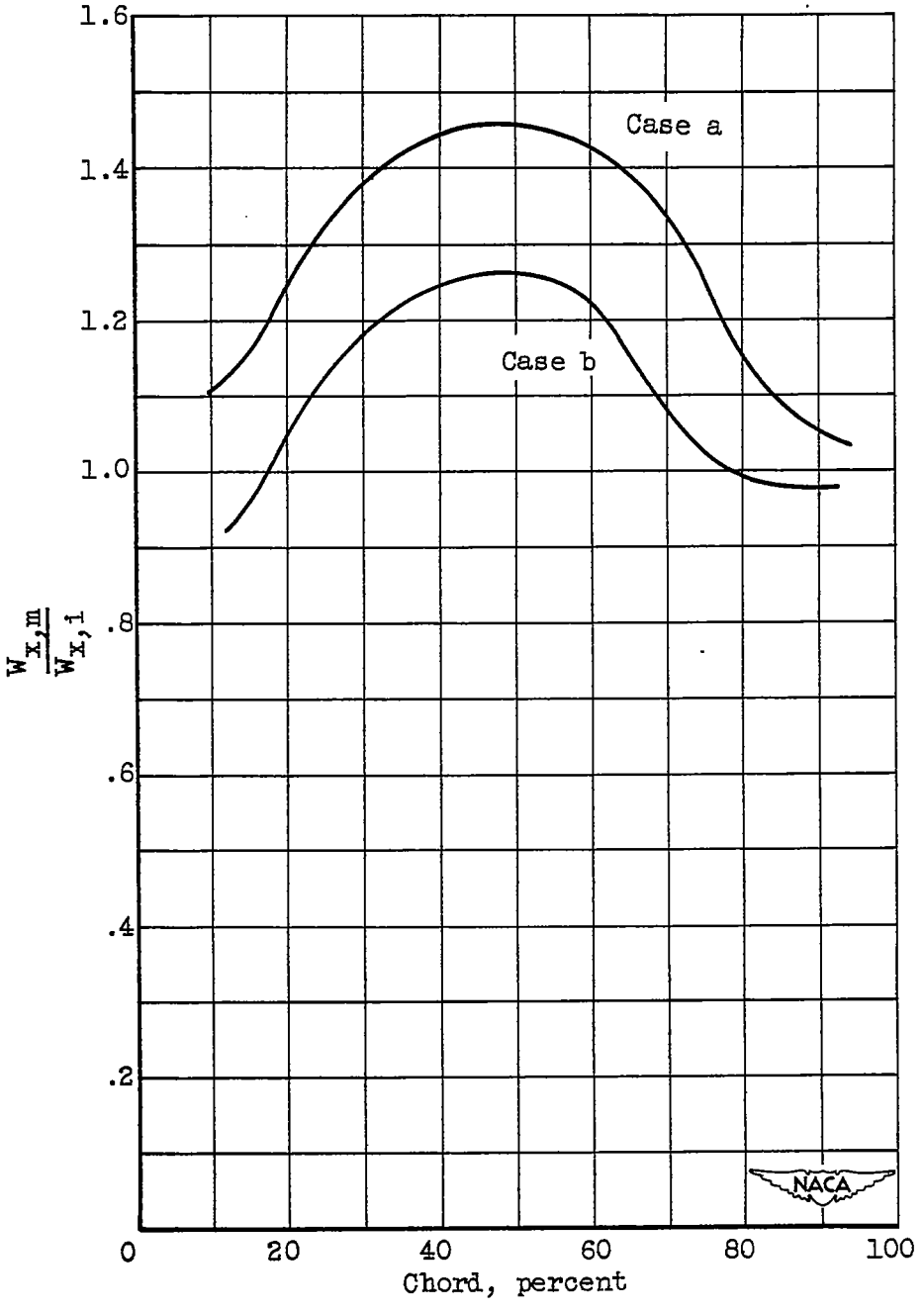

Figure 7. - Variation of axial velocity on mean streamline.

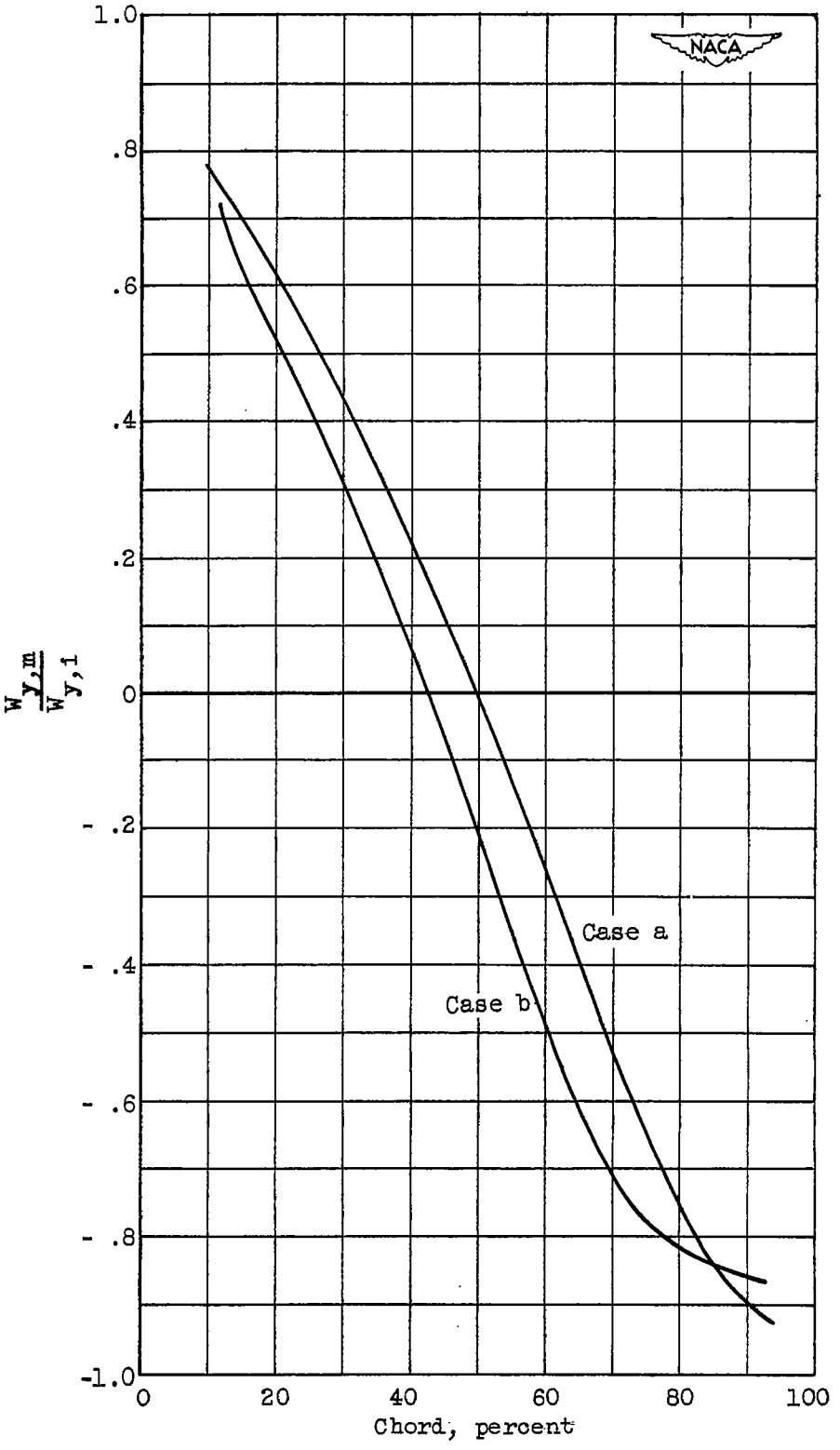

Figure 8. - Variation of tangential velocity on mean streamline.

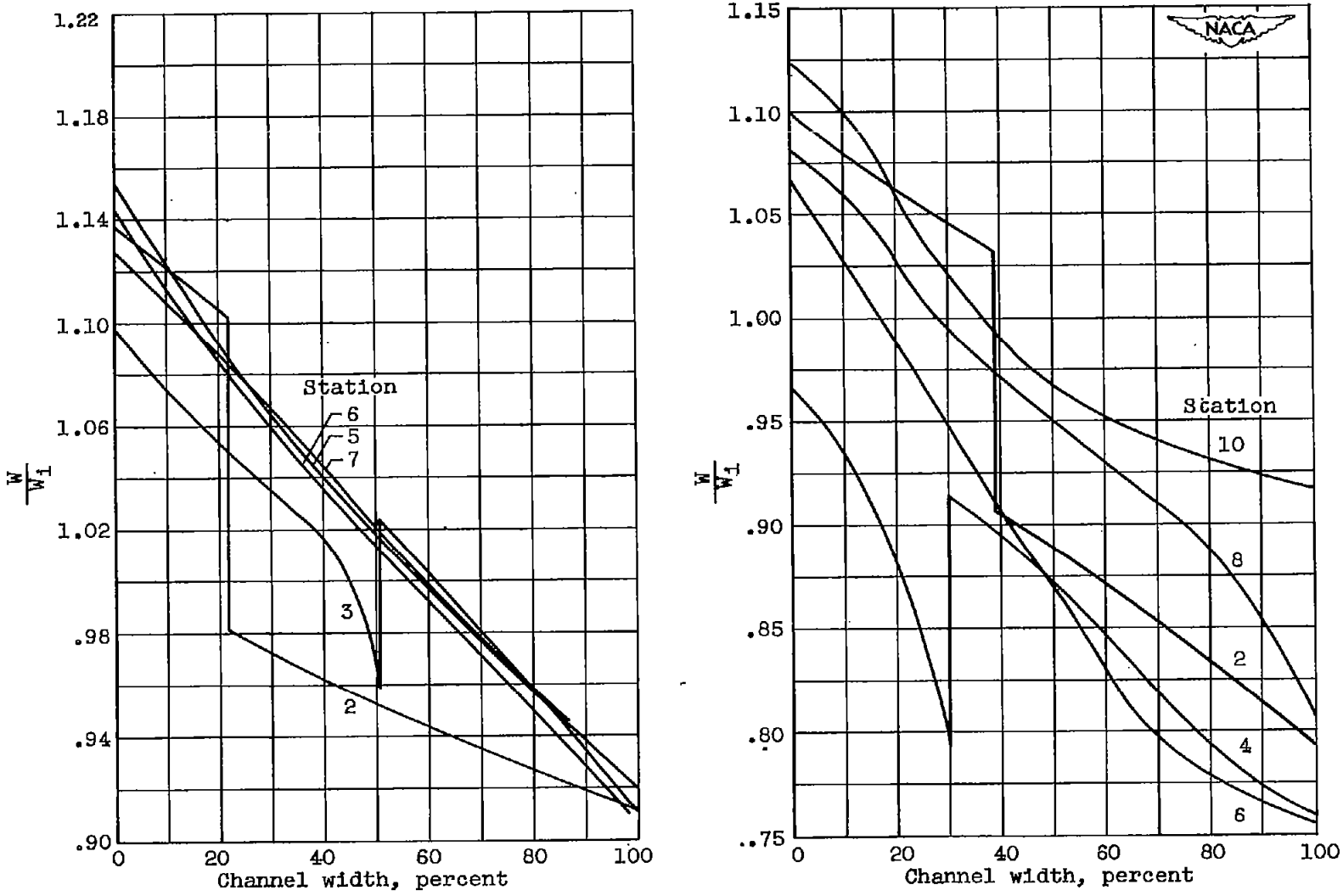

(a) Case a.

(b) Case b.

Figure 9. - Velocity variation across channel.

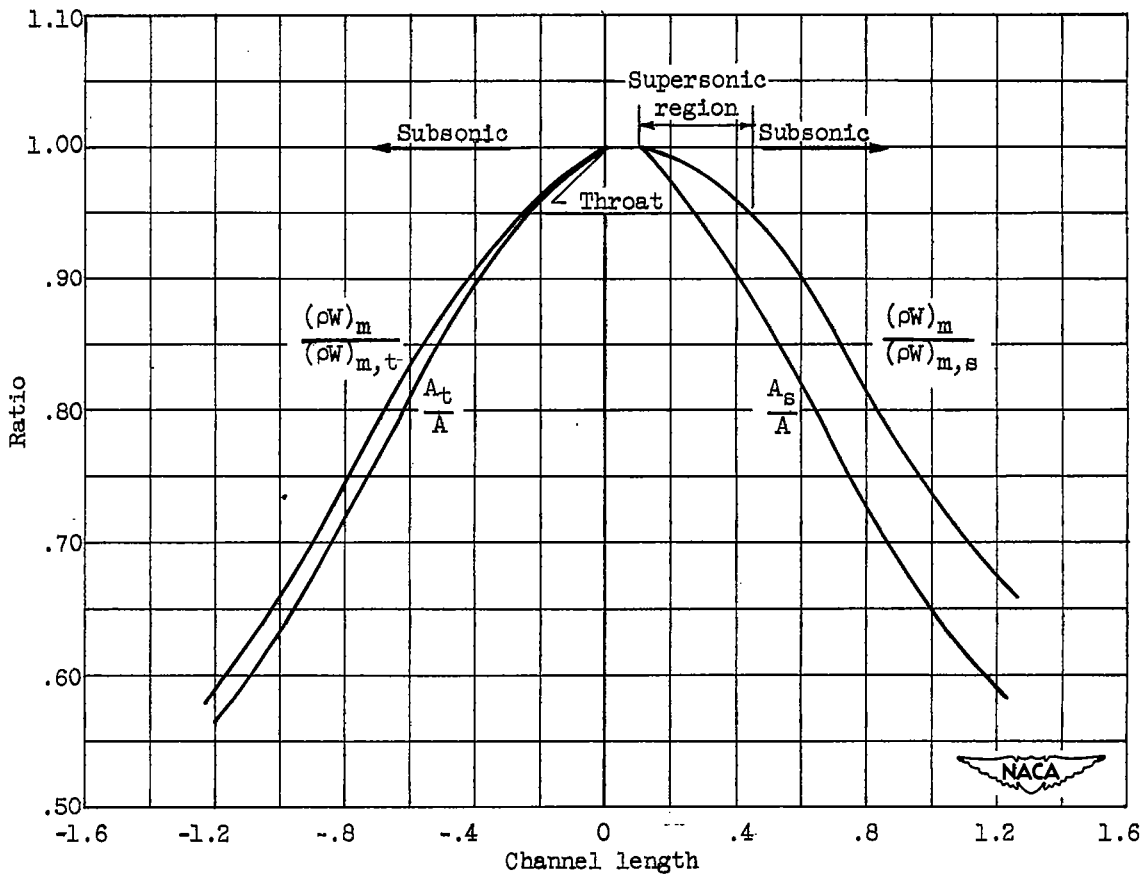

Figure 10. - Comparison of variation in mean specific mass flow and area ratio with short portion of supersonic flow in divergent section.

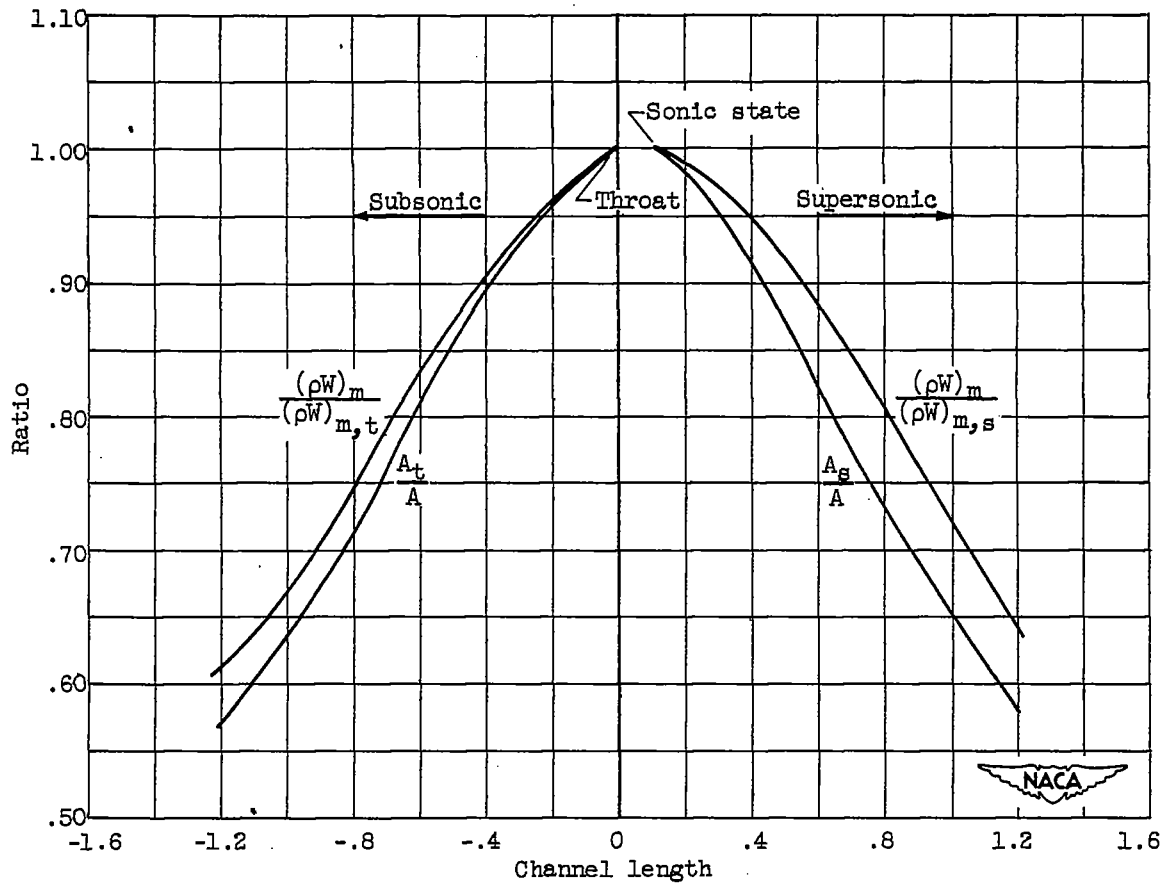

Figure 11. - Comparison of variation in mean specific mass flow and area ratio of nozzle with supersonic flow throughout divergent section.

NACA-Langley - 9-25-51 - 1000